Journal of Saudi Chemical Society (2016) xxx, xxx–xxx

King Saud University

Journal of Saudi Chemical Society

www.ksu.edu.sa
www.sciencedirect.com

ORIGINAL ARTICLE

# Functionalized carbon nanotube doping of P3HT:PCBM photovoltaic devices for enhancing short circuit current and efficiency

**Rohit Bhatia** [a,*], **Lalit Kumar** [b]

[a] *Division of Sustainable Technology, Rudraksh Prodhyogiki Sangathan, Delhi 110092, India*
[b] *Department of Physics, Hindu College, University of Delhi, Delhi 110007, India*

Received 25 August 2016; revised 29 October 2016; accepted 7 November 2016

**KEYWORDS**

Organic photovoltaic;
P3HT;
PCBM;
MWCNTs;
Aromatic azide

**Abstract** We have successfully functionalized multiwalled carbon nanotubes (MWCNTs) using nitrene approach employing the two aryl azides as a precursor for nitrene generation. The dispersion of functionalized MWCNTs has been enhanced in various organic solvents. These functionalized MWCNTs have been successfully doped in various concentrations in the bulk heterojunction (BHJ) organic photovoltaic (OPV) cells with a poly (3-hexyl thiophene) (P3HT) and [6,6]-phenyl-$C_{61}$-butyric acid methyl ester (PCBM) photoactive blended layer. The incorporation of MWCNTs with aryl functional groups, in active the layer, results in enhanced performance with respect to a reference cell. The maximum power conversion efficiency of 1.86% is achieved with adduct I while in the case of adduct II it gets double to 2.0% in comparison with a reference cell. This improvement in the device performance is attributed to enhanced exciton dissociation and improved charge transport properties due to the formation of a nanotube percolation network in the photoactive composite layer.


## 1. Introduction

In recent years organic photovoltaic (OPV) devices based on electron-donating conjugated polymers and electron-accepting fullerene derivatives have emerged as the potential candidate for low-cost and flexible renewable energy sources [1–3]. When light is incident on the devices, it is absorbed by the polymer and excitons are generated on the polymer chains [4,5]. These excitons then diffuse to the polymer-fullerene interface where they dissociate into electron and hole, and the typical diffusion length is about 10 nm [5]. The most successful used OPV material combination is the composite of poly (3-hexyl thiophene) (P3HT) and [6,6]-phenyl-C61-butyric acid methyl ester (PCBM), which is now used as the model system and has achieved high efficiencies under solar illumination [6,7].

* Corresponding author.
E-mail addresses: bhatia.rohit10@gmail.com (R. Bhatia), lalitkrchauhan@gmail.com (L. Kumar).
Peer review under responsibility of King Saud University.

Production and hosting by Elsevier

http://dx.doi.org/10.1016/j.jscs.2016.11.003
1319-6103 

Please cite this article in press as: R. Bhatia, L. Kumar, Functionalized carbon nanotube doping of P3HT:PCBM photovoltaic devices for enhancing short circuit current and efficiency, Journal of Saudi Chemical Society (2016), http://dx.doi.org/10.1016/j.jscs.2016.11.003

Recently, due to their exceptional charge transport properties and electron acceptor behavior carbon nanotubes (CNT) are incorporated into OPVs by doping them into the P3HT/PCBM photoactive layer to utilize them. In photoactive materials, both single walled carbon nanotubes (SWCNTs) and multiwalled carbon nanotubes (MWCNTs) have been incorporated to enhance device performance [8–15]. The introduction of nanotubes in the photoactive layer significantly increases electron mobility thereby reducing the recombination rate and result in enhancing the OPV device performance. One important problem with these devices is the compatibility of different phases in the photoactive layer, predominantly of the nanotubes, which are insoluble in most of the solvents used to fabricate the devices. This low solubility of nanotubes is the main hindrance in obtaining uniform blends of polymer/-fullerene/nanotubes which lower the performance of devices. The drawback can be overcome by functionalization of nanotube using suitable reagents, which lead to good dispersibility of functionalized product in organic solvents [16–18].

Due to their low cost of synthesis and easy availability, MWCNTs have found increased application in OPV devices. In the literature, there are reports, using the carboxylic acid functionalized MWCNTs (O-MWCNTs) for improved thin film deposition compared with pristine MWCNTs which leads to enhanced power conversion efficiency of OPV cells [19,20]. Due to the chemical functionalization nanotube bundles exfoliate and this leads to improved solubility and processability. The functionalization modifies the chemical and physical properties of nanotubes thereby improving the better interaction between the nanotubes and polymer [21]. The highest power conversion efficiency obtained by doping functionalized MWCNTs to P3HT/PCBM was 2.5% of under AM1.5 illumination [22].

In this communication, we report functionalization of MWCNTs using two aryl azides, which serve as a precursor for nitrene generation. The incorporation of these functionalized adducts in P3HT/PCBM OPV devices in different doping concentrations, results in improved performance compared to standard devices. These functional groups were chosen such that will tend to form more percolation networks with P3HT and PCBM. Also, due to their enhanced solubility these adducts result in the better blend with both P3HT and PCBM, resulting in shorten exciton dissociation pathway and better device performance.

## 2. Materials and methods

Multi-walled carbon nanotubes (MWCNTs) were grown by the Chemical Vapor Deposition (CVD) method. (Poly (3,4-ethylenedioxythiophene): poly (styrene sulfonate) (PEDOT:PSS), Indium tin oxide (ITO), regioregular poly (3-hexylthiophene) (RR-P3HT), chlorobenzene and thin layer chromatography TLC plates were purchased from Sigma-Aldrich. All the chemicals were used without any purification. Acetone, petroleum ether, 1, 2, dichlorobenzene, dimethylformamide and diethyl ether were purchased locally. All chemicals used were of AR grade.

High-resolution transmission electron microscopy (HR-TEM) was recorded on TECNAI 300 at 300 kV, and Infra red spectra were recorded on Perkin Elmer spectrum 2000 FTIR spectrometer using KBr pellet in range 400–4000 $cm^{-1}$. Raman spectra were recorded on Renishaw in via Raman microscope with a polarized laser at 514 nm. Thermal gravimetric analysis (TGA) was recorded on Perkin Elmer Model TGA-7, USA, in nitrogen at a heating rate of 10 °C/min from 20 to 800 °C. Alumina was used as the reference material with the platinum crucible to carry out the analysis. Fluorescence spectra were recorded on Varian and UV-Vis-NIR spectra were recorded on a UV-1601 Shimadzu instrument in the range 200–1100 nm.

### 2.1. General procedure for the functionalization of nanotubes

It has been reported previously that pre-treating MWCNTs with microwave irradiation leads to a better degree of functionalization; therefore, the MWCNTs were pre-treated with microwave irradiation before covalent modification reaction. In general, 10 mg of the dried material was taken in the reaction vial and subjected to the microwave irradiation in the domestic microwave oven at 100 W for 15 min with 3 min on and one min off cycle.

For covalent functionalization reaction 10 mg of microwave-treated MWCNTs was suspended in a three neck flask with 10 ml of ortho-dichlorobenzene (ODCB) as a solvent and sonicated for the six hours and after that reaction vessel was placed in a pre-heated oil bath at 180 °C (Fig. 1). In another test tube, 110 mg of azide was dissolved in 5 ml of chlorobenzene and added slowly with the help of a syringe to the reaction vessel over a period of one hour. The inert atmosphere was maintained throughout using nitrogen.

The progress of the reaction was monitored using TLC plates for checking decomposition of azide. After four hours no azide could be detected and the reaction was quenched by removing it from heat. The reaction mixture was then allowed to cool to room temperature and subjected to centrifugation to remove carbon nanotubes, which had not reacted or been only partially functionalized at 2000 rpm. The supernatant was collected and product was precipitated using acetone. The precipitated product was collected by centrifuging at 100,000*g*. The pellet was washed repeatedly with Millipore water, and the final product (3 mg) was dried in the oven at 70 °C.

### 2.2. Fabrication and characterization of photovoltaic cells

The chemically functionalized MWCNTs have been incorporated in the blend of P3HT/PCBM (1:1) in different doping concentrations (1–5%). In the photoactive layer for OPVs, modified MWCNTs of required doping concentration were first dispersed in 1 ml of chlorobenzene and sonicated for 4 h. Then 15 mg of P3HT was added to all solutions, and stirred for 3 h and 15 mg of PCBM was added to the P3HT/MWCNT mixture. These mixtures were stirred overnight and deposited on plasma oxidized ITO/Glass substrates. The spin-coated thin films were allowed to dry for about 40 min at room temperature and then annealed at 125 °C for 10 min. This whole process was carried out in a nitrogen filled glove box. The hole blocking layer bathocuproine (BCP) and the aluminum (Al) electrode were thermally evaporated using a shadow mask under vacuum at the rate of 2 Å/s and 3 Å/s, respectively. Immediately after the device fabrication (Fig. 2), current-voltage measurements were collected using a Keithley 2425 source meter exposing the devices to a 300 W Xe Arc

Please cite this article in press as: R. Bhatia, L. Kumar, Functionalized carbon nanotube doping of P3HT:PCBM photovoltaic devices for enhancing short circuit current and efficiency, Journal of Saudi Chemical Society (2016), http://dx.doi.org/10.1016/j.jscs.2016.11.003

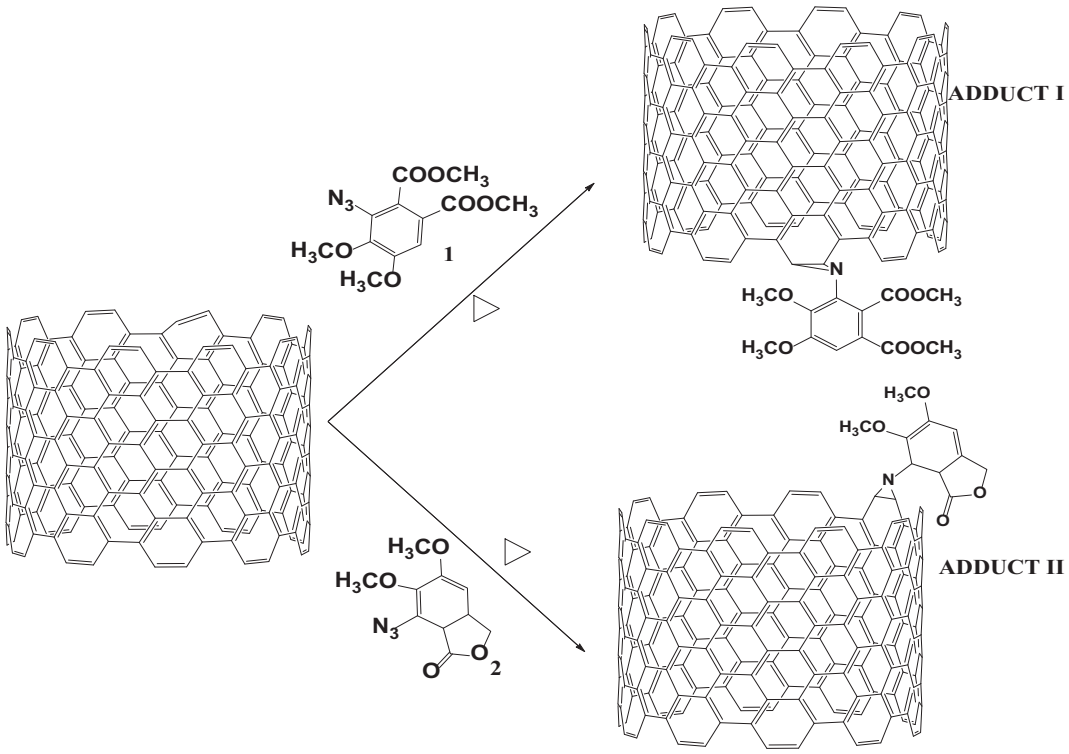


**Figure 1** Functionalization of MWCNTs with aryl azide.

lamp ORIEL simulator, fitted with an Air Mass 1.5 Global (AM 1.5G) filter, calibrated to an intensity of 1000 W $m^{-2}$.

## 3. Results and discussion

Aryl azides 1 and 2 were used to functionalize the MWCNTs. The products thus obtained were characterized with the help of different techniques, discussed below, to confirm that covalent functionalization had taken place successfully.

### *3.1. FT-IR spectroscopy*

FT-IR spectroscopy was used to confirm that functionalization had taken place successfully. It is well known that MWCNTs do not absorb much in the infrared region. In the pristine MWCNTs spectrum (Fig. 3A), we observed asymmetric methyl stretching band at 2960 $cm^{-1}$. The asymmetric methylene stretching band was observed at 2920 $cm^{-1}$ and symmetric methylene stretching band was observed at 2850 $cm^{-1}$. We, also, observed band for C—O stretch mode at 1180 $cm^{-1}$ and for asymmetric stretching bands for C—O at 1151 $cm^{-1}$ and 1080 $cm^{-1}$ which are associated with ether type groups present in pristine MWCNTs.

When successful covalent functionalization of the side wall of carbon nanotube takes place this results in the emergence of new peaks in the spectra of the adducts. In the case of adducts I and II, two important peaks were monitored in FT-IR spectra: (1) the peak around the 2100 $cm^{-1}$ for azide group and (2) peaks for the carbonyl in the region of 1700–1800 $cm^{-1}$.

In the case of MWCNT adduct I, no peak was observed at 2100 $cm^{-1}$ which indicates complete conversion of the azide into the nitrene intermediate, which then attacks the side wall

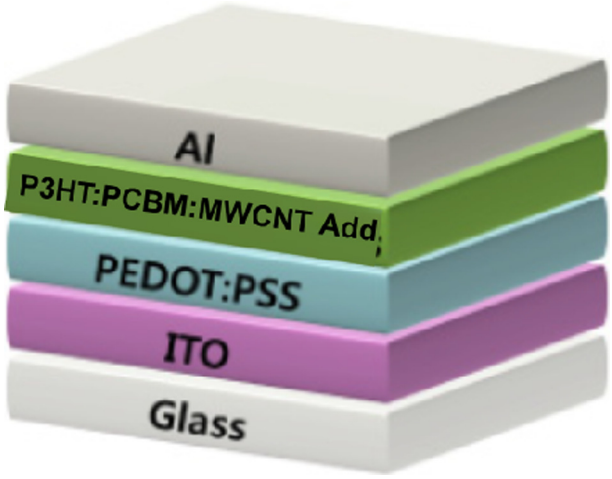


**Figure 2** The structure of the fabricated organic photovoltaic cell.

of carbon nanotubes. Further, a strong peak observed at 1733 $cm^{-1}$ (Fig. 3B) is assigned to a carbonyl functional group which is present in the aryl azide unit. No oxidation with $HNO_3$ was done in our methodology. The band for the carbonyl group confirms successful functionalization. The strong peaks observed at 1254 and 1139 $cm^{-1}$ could be assigned to C—O stretch and out of plane deformation, respectively. The strong peak at 1598 $cm^{-1}$ can be attributed to the C=C stretching of the benzene ring. This evidence shows that the aromatic ring is attached to the MWCNTs.

Similarly, in the case of adduct II, no peak was observed at 2100 $cm^{-1}$ which again indicates complete decomposition of

Please cite this article in press as: R. Bhatia, L. Kumar, Functionalized carbon nanotube doping of P3HT:PCBM photovoltaic devices for enhancing short circuit current and efficiency, Journal of Saudi Chemical Society (2016), http://dx.doi.org/10.1016/j.jscs.2016.11.003

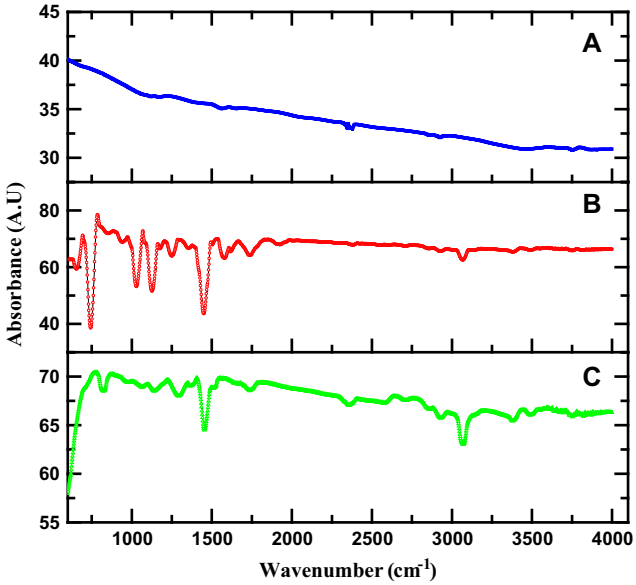


**Figure 3** FT-IR spectra of (A) pristine MWCNTs, (B) MWCNT adduct I and (C) MWCNT adduct II.

the azide group. A strong peak for the carbonyl functional group was observed at 1728 $cm^{-1}$ in the case of adduct II (Fig. 3C), which can be assigned to the carbonyl of lactone ring present in aryl azide 2.

Characteristic peaks for the aromatic ring were observed in the range 1400–1640 $cm^{-1}$. A strong peak at the 1637 $cm^{-1}$ could be assigned as C═C stretching of the benzene ring. Peaks at 1243 and 1156 $cm^{-1}$ were assigned to C—O stretch and out-of-plane deformation, respectively. Further, the peak for C—H bending was observed at 836 $cm^{-1}$. All these evidences indicate toward successful covalent functionalization of MWCNTs.

### 3.2. UV-Vis spectroscopy

UV-Vis spectrum of pristine MWCNTs does not show any well define peaks, but background absorption can be observed in the spectra due to the presence of bundles of carbon nanotubes. In comparison with this, the UV-Vis spectrum of adduct I (Fig. 4A) shows an intense peak at 280 nm which is due to the n-$\pi^*$ electron transition in the aromatic chromophore. The high intensity of the peak can be attributed to the high degree of functionalization, due to a large number of chromophore are present on the carbon nanotube. In U. V.-Vis spectrum of MWCNT adduct II (Fig. 4A) two well-defined peaks were observed that were not present in the spectrum of the starting MWCNTs, one at 280 nm and the other at the 350 nm. The peak at 280 nm is due to the n-$\pi^*$ transition of the aromatic chromophore and the peak at 350 nm can be assigned due to $\pi$-$\pi^*$ transitions between the carbon nanotube and the aromatic ring.

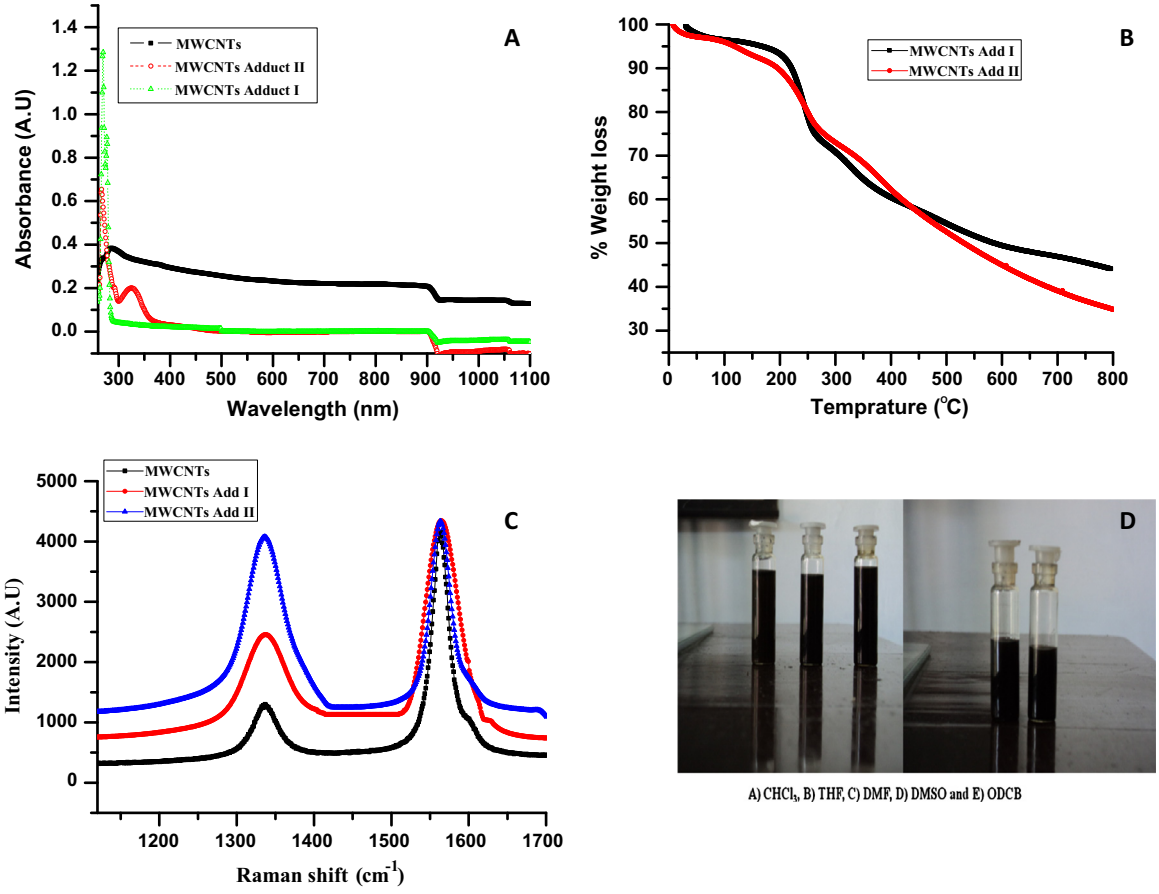


**Figure 4** (A) UV-Vis studies, (B) TGA studies, (C) Raman studies and (D) solubility in common solvent of MWCNT adducts I and II.

### 3.3. Thermal gravimetric analysis (TGA)

Thermal gravimetric analysis has been used extensively to determine the degree of functionalization in SWCNTs, but this technique is less informative in case of MWCNTs, still it can reflect the degree of functionalization. The pristine MWCNTs show an overall loss of 4% under the inert condition of heating, as spectra are recorded under a nitrogen atmosphere, this mass loss cannot be attributed due to combustion, but this may be due to the organic and inorganic impurities (including organic solvents) trapped in MWCNTs. In the case of MWCNT adduct I (Fig. 4B), the first major loss after 100 °C was observed, which finishes at 300 °C.

This loss can be attributed to the loss of organic group attached to the side wall of the carbon nanotubes. The second loss starts after 300 °C and finishes at 400 °C. This may be due to the loss of carbonyl groups which are present in the functional group attached to the side wall. Total mass loss till 400 °C was 54.43%. After 400 °C no significant mass loss was observed. Similarly, for the MWCNT adduct, II total mass of 65% (Fig. 4B) was observed before 400 °C, which can be attributed to the reasons cited above. From both these observations, it is confirmed that successful covalent functionalization of carbon nanotube has taken place.

### 3.4. Raman spectroscopy

In pristine MWCNTs used in this study, D band was observed at 1336 $cm^{-1}$ and G band was observed at 1561 $cm^{-1}$. The intensity ratio ($I_D/I_G$) for starting MWCNTs was 0.30. After functionalization in the case of adduct 1 (Fig. 4C), an increase in D band intensity was observed. This increase in intensity can be attributed to the increase in the defects in carbon nanotubes due to functionalization. After functionalization due to a covalent functionalization, a large number of the $sp^2$ carbon get converted to the $sp^3$ which could lead to the increase in the D band intensity. Also the intensity ratio ($I_D/I_G$) in the case of adduct I increases to 0.60 after functionalization.

In case of adduct II (Fig. 4C) similar to adduct I increases in the D band intensity were observed, but in this case the increase is more than adduct I. This increase in D band intensity can be attributed to conversion of $sp^2$ hybridized carbon to $sp^3$ hybridization due to the formation of covalent bond on insertion reaction. In adduct II, the intensity ratio is 0.93, indicating higher functionalization in adduct II. This observation is also supported by the TGA studies, where the more mass loss was observed in the case of adduct II than for adduct I. In both adducts improvement in the intensity ratio combined with an increase in D band intensity was observed, pointing toward the successful covalent functionalization of MWCNTs with aryl azide. The functionalized material is more easily dispersed in common organic solvents (Fig. 4D) in comparison with the pristine MWCNTs.

### 3.5. Transmission electron microscope (TEM)

Transmission electron microscope (TEM) has emerged as a major tool for nanoscale morphological visualization of carbon nanotubes. The HR-TEM image of pristine MWCNTs shows the presence of super bundles (Fig. 5A). These super bundles can be attributed to the presence of van der Waals forces interaction between tubes.

After functionalization, no super bundles are observed in the TEM images (Fig. 5B). Functionalized adducts show a clear change in the morphology. In both the adducts it is observed that carbon nanotubes were present in smaller bundles, indicating that due to functionalization the strong van der Waal forces of attraction between the tubes is disturbed, which results in breaking of super bundles into smaller bundles, increasing solubility in common organic solvents.

This again indicates toward that successful functionalization of MWCNTs has taken place using aryl azides I and II. Further, in TEM images it is observed that morphology carbon nanotubes were changed after functionalization which is highlighted by the red arrow (Fig. 5), and this may be due to high degree of functionalization.

### 3.6. Photovoltaic studies

As discussed earlier that the functionalized MWCNTs can be used for photovoltaic application with enhanced efficiency, therefore various functionalized MWCNT adducts were used in doping concentration to see how they improve the photovoltaic properties of P3HT: PCBM devices. To understand how functionalized MWCNT adducts interact with the conducting polymer P3HT, FT-IR spectroscopy studies were undertaken. From these studies, the molecular level interaction between the P3HT and MWCNT adducts is discernible (Fig. 6). Broadening of the FT-IR peaks was observed after mixing of MWCNT adducts in the P3HT. Further pronounced

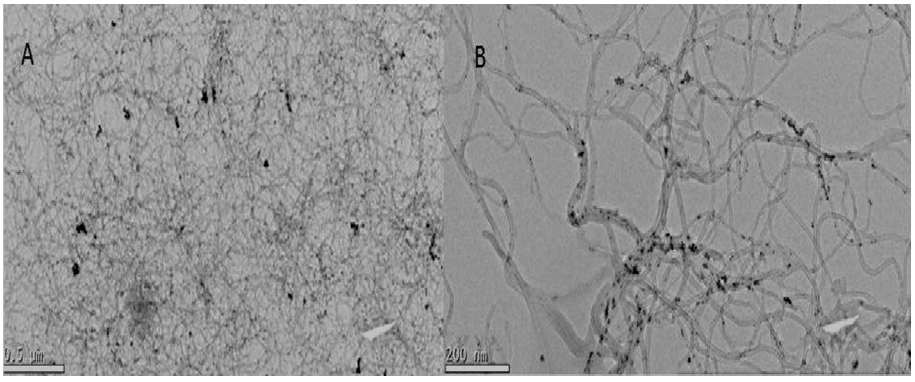


**Figure 5A** HR-TEM image of pristine MWCNTs at different resolutions: (A) 500 nm and (B) 200 nm.

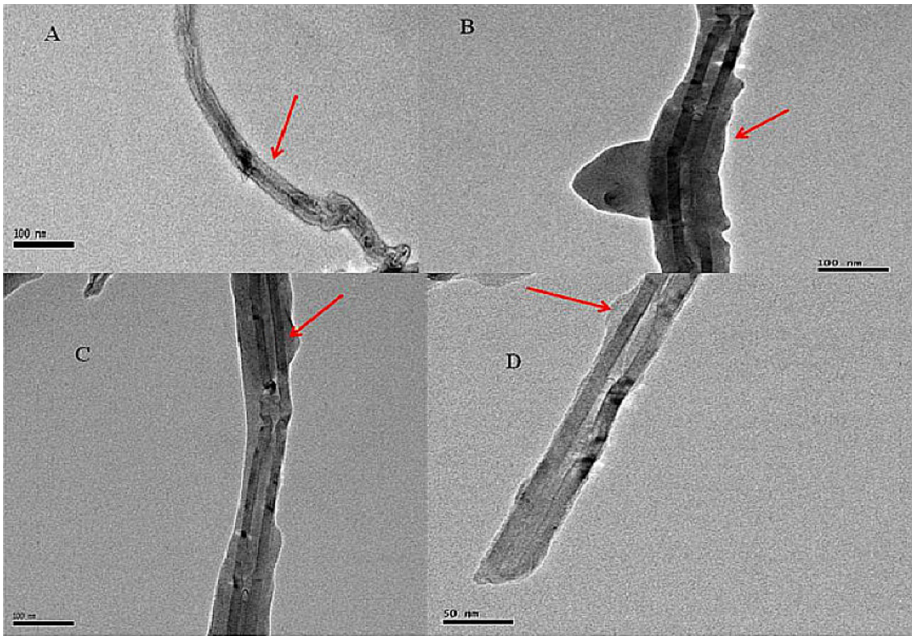


**Figure 5B** TEM images of MWCNT adduct I (A and B) and MWCNT adduct II (C and D).

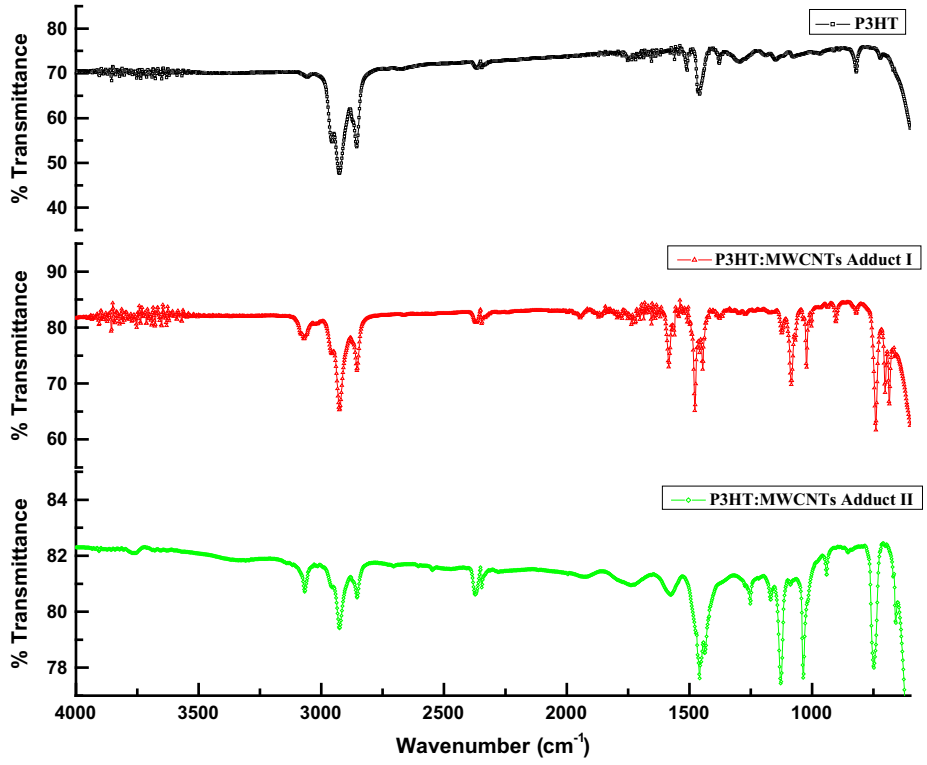


**Figure 6** FT-IR spectra of P3HT and MWCNT adducts.

changes were observed in the aromatic C—H stretching, vibration region, and peaks in this region become strong and broad in comparison with the P3HT. This change in intensity can be attributed to the π-π interaction between P3HT and MWCNT adducts containing the aromatic ring on the side walls of carbon nanotubes. Further, three new strong peaks were observed in P3HT-MWCNT adduct composites, which could be assigned to C—C bonds in MWCNTs.

In region 1700–1800 $cm^{-1}$ spectra of P3HT and MWCNT adduct peaks, were observed, which were assigned to the C═O in conjugation with C═C after functionalization. In the spectra of composites, peaks due to P3HT remain visible,

Please cite this article in press as: R. Bhatia, L. Kumar, Functionalized carbon nanotube doping of P3HT:PCBM photovoltaic devices for enhancing short circuit current and efficiency, Journal of Saudi Chemical Society (2016), http://dx.doi.org/10.1016/j.jscs.2016.11.003

and peaks around 1510–1530 $cm^{-1}$ and 1450–1470 $cm^{-1}$ were associated with symmetric and asymmetric ring stretching vibrations, respectively. Their relative ratio indicate the conjugation length of the polymer. The peaks arising due to the C=C stretching around 1200–1500 $cm^{-1}$ in the spectra of the composite film become broad and of medium intensity in comparison with the P3HT.

To further study the molecular level interaction between P3HT and MWCNT adducts I and II, we used UV-Vis spectroscopy studies. In UV-Vis spectra we observed that with in increase concentration of MWCNT adduct I their is increase absorption intensity in region 480–530 nm (Fig. 7A). This increase in the intensity of P3HT can attribute to the more ordered vibronic structure of P3HT due to doping of MWCNT adduct, which is consistent with earlier reports [23] and this increase in intensity can also be explained in terms of self-assembly of P3HT around the MWCNTs backbone which results in more ordered structure of polymer and results in increased absorption intensity. Further increase in absorption intensity is observed near 600 nm with the maximum in the case of 5% doping. This can be attributed to partial crystallization of the conjugated polymer, which is due to the non-covalent interaction between MWCNT adduct and polymer [24].

In the case of UV-Vis spectrum of MWCNT adduct II (Fig. 7B), a similar trend is observed to that in the case of MWCNT adduct I, the only difference being that increase in absorption intensity is less than that of MWCNT adduct I.

The PL signature for P3HT at 575 nm corresponds to the $\pi$-$\pi^*$ band due to electronic transitions in P3HT and the shoulder around 630 nm corresponds to the radiative decay of excitons between the intermediate states of the polymer [10,25]. A significant reduction in the PL intensity of the P3HT luminescence peaks was observed when MWCNT adducts I and II are added to it (Fig. 7C and D). This reduction in photoluminescence can be attributed to the photoinduced charge separation between electron donating (P3HT) and electron accepting (MWCNT adduct) molecules [26].

The addition of MWCNT adducts leads to the formation of heterojunctions between the carbon nanotube and P3HT, which leads to the quenching of luminescence. In addition to the radiative recombination, non-radiative recombination in the form of Auger recombination and thermalization are expected in all the blends which can affect the photovoltaic parameters of devices fabricated using these blends. The shape of the PL emission spectra is preserved in all doping concentrations, indicating that radiative recombination processes remain similar, but at different intensities, for all the concentrations studied.

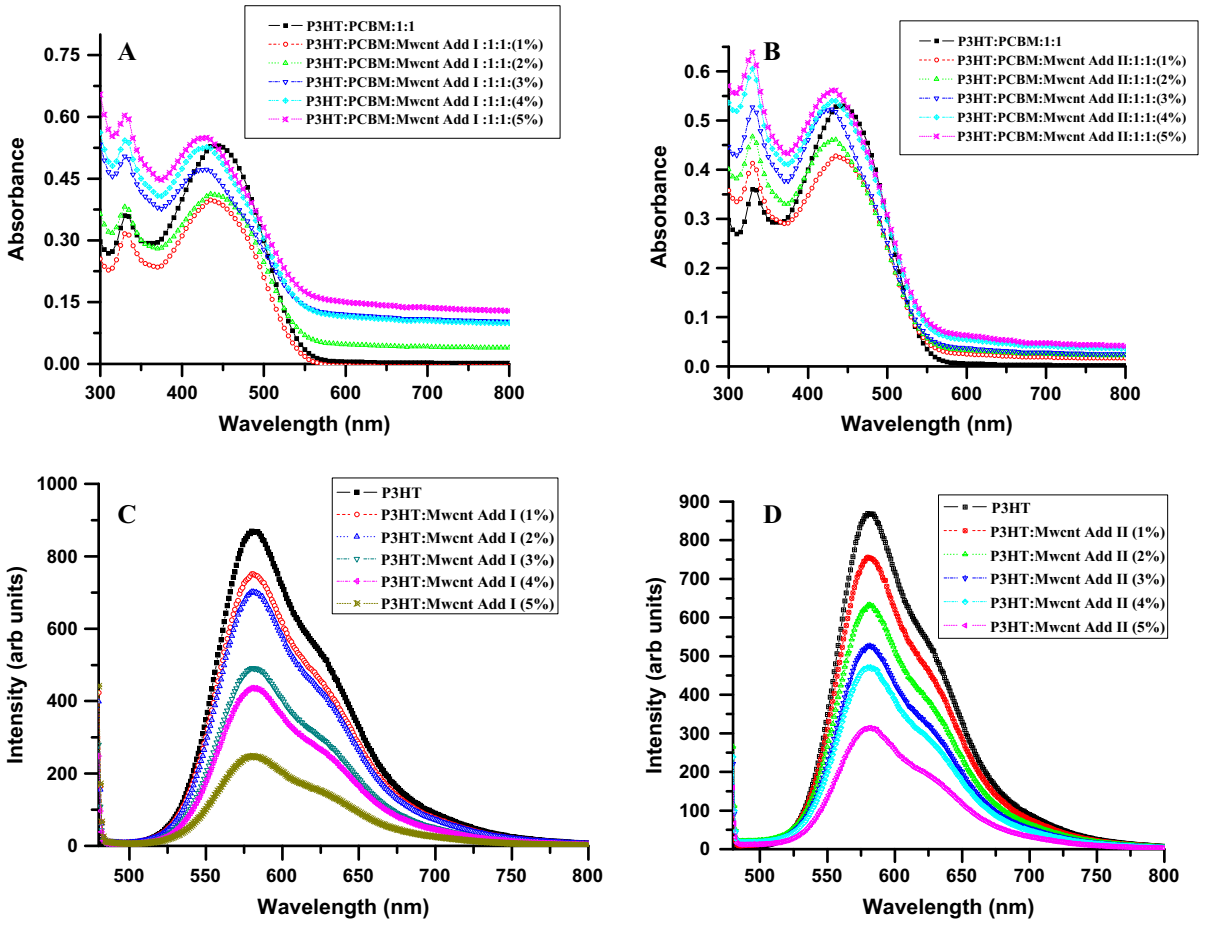


**Figure 7** UV-Vis (A and B) and photoluminescence (PL) (C and D) spectra of P3HT with different concentrations of MWCNT adducts I and II.

Based on the above results these functionalized MWCNTs were used for fabrication of photovoltaics devices. *J-V* characteristic of unoptimized photovoltaic devices fabricated using the MWCNT adducts I and II is shown in Fig. 8. From the *J-V* curve, it can be observed that device fabricated using P3HT: PCBM: MWCNT adduct I composite shows enhancement in the fundamental device parameters in comparison with standard P3HT: PCBM devices, which is consistent with earlier reports [10,25]. The concentration of carbon nanotubes in the active layer governs the performance of the devices and best device characteristics were found at 4% doping concentration by weight, for the D/A loading in case of adduct I.

The open-circuit voltage ($V_{oc}$) corresponds to the amount of forward bias in the solar cell due to the bias of the solar cell junction with the light-generated current. In devices fabricated using the MWCNT adduct I, $V_{oc}$ of the standard cell was 0.53 V. A marginal increase in the $V_{oc}$ was observed at concentrations 1%, 2% and 5% and $V_{oc}$ decreases marginally at concentrations 2% and 4% (Fig. 9A). This marginal change in open circuit voltage indicates that in all the devices incorporation of

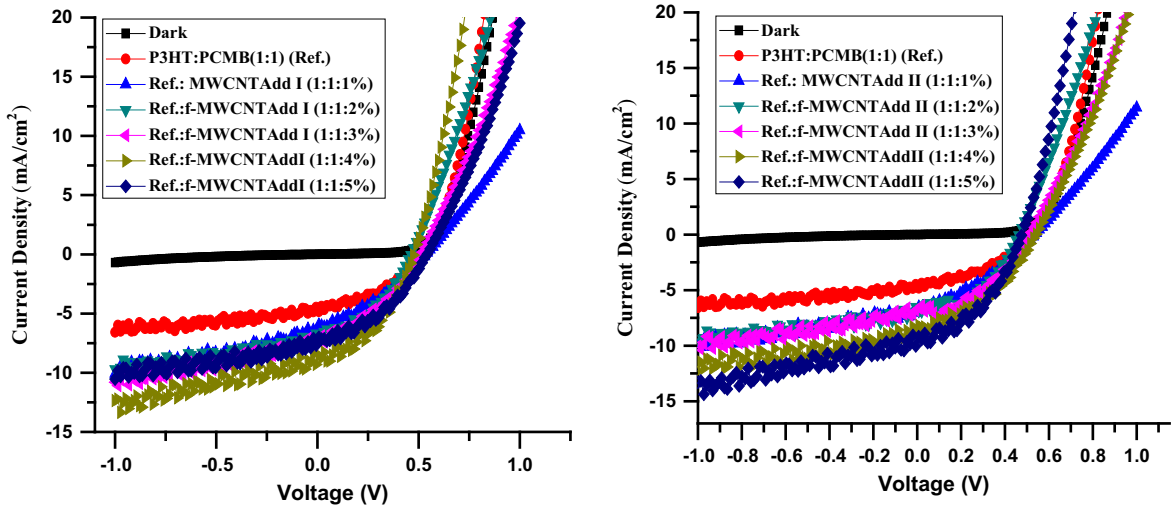


**Figure 8** *J–V* characteristics for the MWCNT adducts I and II, in dark and under AM 1.5 illumination.

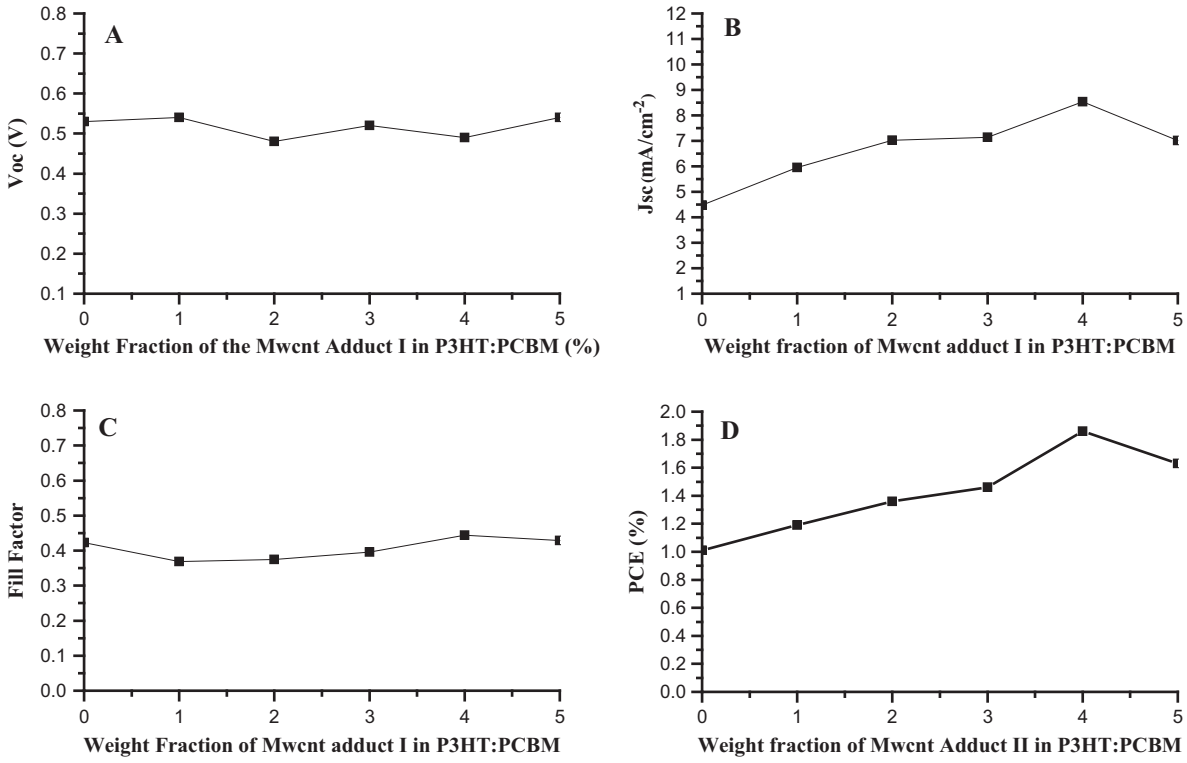


**Figure 9** Experimental value of (A) open-circuit voltage ($V_{oc}$), (B) short-circuit current ($J_{sc}$), (C) fill factor (FF) and (D) efficiency as a function of the MWCNT adduct I.

MWCNT adduct I does not interfere with the heterojunctions between the P3HT/PCBM and therefore no major change in the $V_{oc}$ is observed.

The short-circuit current ($J_{sc}$) is the current through the solar cell when the voltage across the solar cell is zero (i.e., when the solar cell is short circuited). Since the short circuit current ($I_{sc}$) is roughly proportional to the area of the solar cell, the short circuit current density, $J_{sc} = I_{sc}/A$, is often used to compare solar cells. Short circuit current density ($J_{sc}$) in all the devices shows improvement in comparison with the standard devices (Fig. 9B).

The $J_{sc}$ show a dependency on the molecular weight of the donor, which affects the microstructure formation at spin casting. The standard P3HT: PCBM device has a $J_{sc} = 4.48$ mA cm$^{-2}$ and $J_{sc}$ of the device based on MWCNT adduct I show an improvement with maximum $J_{sc}$ of 8.53 mA cm$^{-2}$ is observed at 4% doping concentration by weight in P3HT: PCBM. A decrease in the $J_{sc}$ value was observed at doping concentration 5% weight of MWCNT adduct I in P3HT: PCBM

Fill factor (FF) is defined as the ratio of the maximum power from the solar cell to the product of $V_{oc}$ and $I_{sc}$. Devices fabricated using the MWCNT adduct I show an interesting trend regarding the Fill Factor. It increases with increased concentration of MWCNT adduct I reaching a maximum at a concentration of 4% weight in P3HT: PCBM (Fig. 9C).

After reaching a maximum at 4% of adduct the Fill factor again decreases, but it is still higher than that for the standard

**Table 1** Photovoltaic parameters of device doped with various concentrations of the MWCNT adduct in P3HT: PCBM.

| Cell | VOC (V) | JSC (mA/cm$^2$) | FF | Efficiency $\eta$ (%) |
|---|---|---|---|---|
| P3HT:PCBM (X) | 0.53 | 4.48 | 0.423 | 1.01 |
| X + f-MWCNT I (1%) | 0.54 | 4.48 | 0.423 | 1.01 |
| X + f-MWCNT I (2%) | 0.49 | 5.95 | 0.369 | 1.19 |
| X + f-MWCNT I (3%) | 0.52 | 7.02 | 0.375 | 1.36 |
| X + f-MWCNT I (4%) | 0.48 | 7.14 | 0.396 | 1.46 |
| X + f-MWCNT I (5%) | 0.54 | 8.53 | 0.444 | 1.86 |
| X + f-MWCNT II (1%) | 0.53 | 6.49 | 0.378 | 1.30 |
| X + f-MWCNT II (2%) | 0.51 | 6.63 | 0.448 | 1.53 |
| X + f-MWCNT II (3%) | 0.48 | 6.86 | 0.472 | 1.58 |
| X + f-MWCNT II (4%) | 0.54 | 8.18 | 0.430 | 1.89 |
| X + f-MWCNT II (5%) | 0.49 | 9.18 | 0.422 | 2.00 |

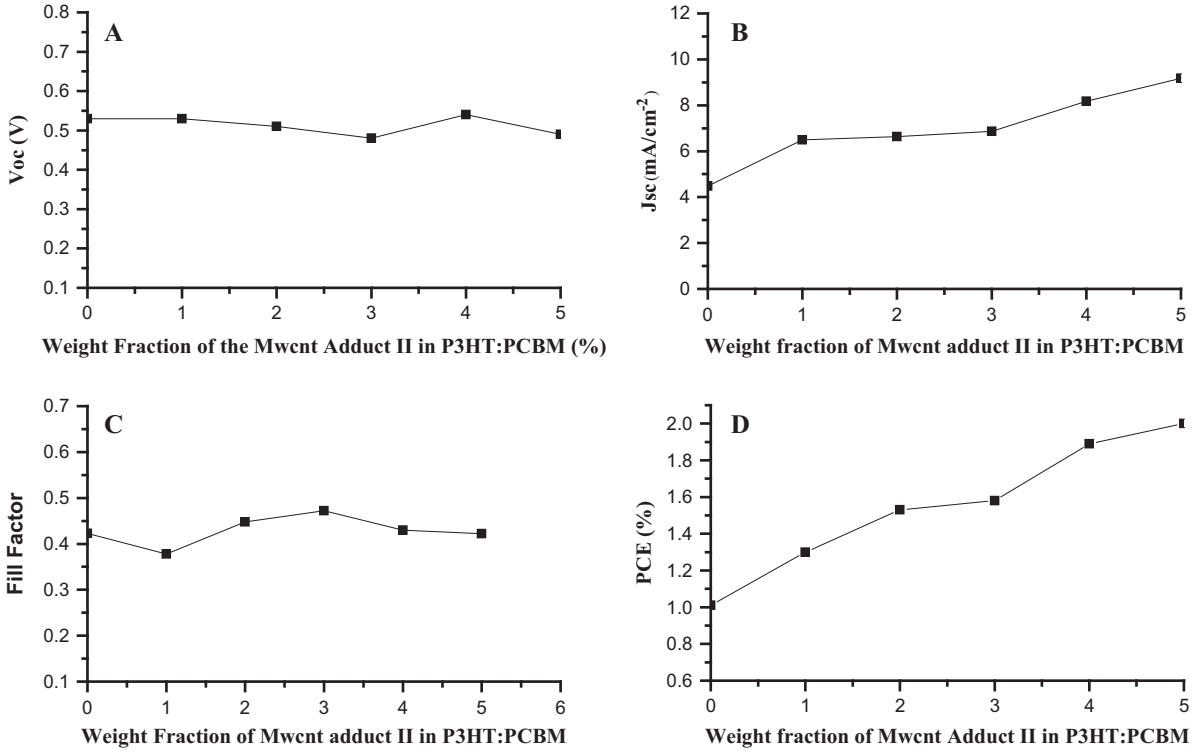


**Figure 10** Experimental value of (A) open-circuit voltage ($V_{oc}$), (B) short-circuit current ($J_{sc}$), (C) fill factor (FF) and (D) efficiency as a function of the MWCNT adduct II.

Please cite this article in press as: R. Bhatia, L. Kumar, Functionalized carbon nanotube doping of P3HT:PCBM photovoltaic devices for enhancing short circuit current and efficiency, Journal of Saudi Chemical Society (2016), http://dx.doi.org/10.1016/j.jscs.2016.11.003

P3HT: PCBM cell. The Fill factor of the devices depends on the polymer–metal interface morphology and the mobility of electron in the semiconducting layer [26,27]. Photo Conversion Efficiency (PCE) is defined as the ratio of energy output from the solar cell to input energy from the sun. The efficiency of a solar cell is determined as the fraction of incident power which is converted to electricity and is defined as follows:

$$\eta = J_{sc} \cdot V_{oc} \cdot FF/P_s$$

As discussed above doping of the MWCNT adduct I leads to the improvement in $J_{sc}$ and the Fill factor which results in the improvement in overall efficiencies of devices (Fig. 9D). It can be observed that as the concentration of adduct is increased, there is an increase in the efficiency of the device. This increase in efficiency can be attributed to the increase in the $J_{sc}$ of the device containing the MWCNT adduct I.

It can thus be concluded, that however $V_{oc}$ of devices do not show much improvement after doping of the MWCNT adduct I. An overall increase in the efficiency is observed due to high $J_{sc}$ and a better fill factor in comparison with the standard P3HT: PCBM devices. Photovoltaic parameters of the devices are shown in Table 1.

Similarly, photovoltaic devices were fabricated using MWCNT adduct II – P3HT-PCBM. Similar to adduct I, no major change was found in the open circuit voltage ($V_{oc}$) of the device fabricated using the adduct II (Fig. 10A), indicating that its addition does not interfere with the heterojunction between the P3HT:PCBM. The Highest $V_{oc}$ of 0.54 V was observed at a concentration of 4% by weight in P3HT: PCBM and lowest value of 0.48 V was observed at 3% concentration of MWCNT adduct II in P3HT: PCBM.

Short circuit current density ($J_{sc}$) show similar trends to that of adduct I i.e. it increases with an increase in the concentration of MWCNT adduct II (Fig. 10B). The highest $J_{sc}$ was observed at a doping concentration of 5% in P3HT: PCBM and lowest was observed at a doping concentration of 1% in P3HT: PCBM.

Fill factor (FF) of the device doped with MWCNT adduct II showed improvement with an increase in concentration (Fig. 10C), and highest FF of 0.472 was observed for a doping concentration of 3%. The slight decrease in the FF is observed for doping concentration 4% and 5% but this is still high in comparison with the standard devices.

Doping of MWCNT adduct II does not improve the $V_{oc}$ much but leads to a considerable improvement in the $J_{sc}$ and FF. This improvement leads to considerable enhancement in the device efficiency with the highest efficiency of 2% being observed at a doping concentration of 5% of adduct II in P3HT: PCBM (Fig. 10D), which is a onefold increase in the efficiency of the standard devices of P3HT: PCBM.

Doping of carbon nanotubes increases the current density in the devices, thereby improving the efficiency of the devices. Photovoltaic parameters of the devices fabricated using the MWCNT adduct II are summarized in Table 1.

## 4. Conclusions

Multi-walled carbon nanotubes (MWCNTs) are more complex compared to the single walled carbon nanotubes but are easier to prepare and relatively inexpensive. The lack of solubility of MWCNTs however, hampers their use in large scale application. MWCNTs have been functionalized using two aryl azides 1 and 2. These adducts thus obtained have been characterized using FT-IR, UV-Vis, Raman spectroscopy, TGA and TEM studies. These adducts are soluble in most common organic solvents. The same have been successfully used for photovoltaics and the photovoltaic parameters calculated from the $J$–$V$ graph. High $J_{sc}$ values were observed and consequently, an increase in photocurrent efficiency (PCE) has been observed.

## Acknowledgments

I gratefully acknowledge Prof. S.V. Eswaran, Emeritus Scientist, Regional Center for Biotechnology, for providing necessary facility to carry out this work. I also thank Dr. Vinya Gupta, Senior Scientist, CSIR-NPL, for helping with photovoltaic studies.

## References

[1] S.H. Park, A. Roy, S. Beaupre, S. Cho, N. Coates, J.S. Moon, D. Moses, M. Leclerc, K. Lee, A.J. Heeger, Bulk heterojunction solar cells with internal quantum efficiency approaching 100%, Nat. Photonics 3 (2009) 297–302.
[2] G. Yu, J. Gao, J.C. Hemmelen, F. Wudl, A.J. Heeger, Polymer photovoltaic cells: enhanced efficiencies via a network of internal donor-acceptor heterojunctions, Science 270 (1995) 1789–1791.
[3] D. Adikaari, N. Dissanayake, S.R.P. Silva, Hybrid organic-inorganic solar cells: recent developments and outlook, Sel. Top. Quant. Electron. IEEE J. 16 (2010) 1595–1606.
[4] A.L. Ayzner, C.J. Tassone, S.H. Tolbert, B.J. Schwartz, Reappraising the need for bulk heterojunctions in polymer-fullerene photovoltaics: the role of carrier transport in all-solution-processed P3HT/PCBM bilayer solar cells, J. Phys. Chem. C 113 (2009) 20050.
[5] P. Shaw, A. Ruseckas, I. Samuel, Exciton diffusion measurements in poly (3-hexylthiophene), Adv. Mater. 20 (2008) 3516–3520.
[6] G. Li, V. Shrotriya, J. Huang, Y. Yao, T. Moriarity, K. Emery, Y. Yang, High-efficiency solution processable polymer photovoltaic cells by self-organization of polymer blends, Nat. Mater. 4 (2005) 864–868.
[7] J.K. Lee, W.L. Ma, C.J. Brabec, J. Yuen, J.S. Moon, J.K. Kim, K. Lee, G.C. Bazan, A.J. Heeger, Processing additives for improved efficiency from bulk heterojunction solar cells, J. Am. Chem. Soc. 130 (2008) 3619–3623.
[8] E. Kymakis, G.A.J. Amaratunga, Single-wall carbon nanotube/conjugated polymer photovoltaic devices, Appl. Phys. Lett. 80 (2002) 112–114.
[9] E. Kymakis, I. Alexandrou, G.A.J. Amaratunga, High open-circuit voltage photovoltaic devices from carbon-nanotube-polymer composites, J. Appl. Phys. 93 (2003) 1764–1768.
[10] R.A. Hatton, A.J. Miller, S.R.P. Silva, Carbon nanotubes: a multi-functional material for organic optoelectronics, J. Mater. Chem. 18 (2008) 1183–1192.
[11] R.A. Hatton, N.P. Blanchard, L.W. Tan, G. Latini, F. Cacialli, S.R.P. Silva, Oxidised carbon nanotubes as solution processable, high work function hole-extraction layers for organic solar cells, Org. Electron. 10 (2009) 388–395.
[12] A.J. Miller, R.A. Hatton, S.R.P. Silva, Interpenetrating multi-wall carbon nanotube electrodes for organic solar cells, Appl. Phys. Lett. 89 (2006) 133117.

Please cite this article in press as: R. Bhatia, L. Kumar, Functionalized carbon nanotube doping of P3HT:PCBM photovoltaic devices for enhancing short circuit current and efficiency, Journal of Saudi Chemical Society (2016), http://dx.doi.org/10.1016/j.jscs.2016.11.003

[13] A.J. Miller, R.A. Hatton, S.R.P. Silva, A water soluble multi-wall carbon nanotube-polythiophene composite for bi-layer photovoltaics, Appl. Phys. Lett. 89 (2006) 123115.
[14] B. Pradhan, S.K. Batabyal, A.J. Pal, Functionalized carbon nanotubes in donor/acceptor-type photovoltaic devices, Appl. Phys. Lett. 88 (2006) 093106.
[15] S. Berson, R. de Bettignies, S. Bailly, S. Guillerez, B. Jousselme, Elaboration of P3HT/CNT/PCBM composites for organic photovoltaic cells, Adv. Funct. Mater. 17 (2007) 3363–3370.
[16] Y. Wang, H.Z. Chen, H.Y. Li, M. Wang, Fabrication of carbon nanotubes/copper phthalocyanine composites with improved compatibility, Mater. Sci. Eng. B 117 (2005) 296–301.
[17] T. Hasobe, Supramolecular nanoarchitectures for light energy conversion, Phys. Chem. Chem. Phys. 12 (2010) 44–57.
[18] J. Shen, W. Huang, L. Wu, Y. Hu, M. Ye, Study on amino-functionalized multiwalled carbon nanotubes, Mater. Sci. Eng. 464 (2007) 151–156.
[19] J. Chen, M.A. Hamon, H. Hu, Y. Chen, A.M. Rao, P.C. Eklund, R.C. Haddon, Solution properties of single-walled carbon nanotubes, Science 282 (1998) 95–98.
[20] J. Zhang, H. Zou, Q. Qing, Y. Yang, Q. Li, Z. Liu, X. Guo, Z. Du, Effect of chemical oxidation on the structure of single-walled carbon nanotubes, J. Phys. Chem. B 107 (2003) 3712–3718.
[21] M.A. Hamon, H. Hu, B. Zhao, P. Bhowmik, R. Sen, M.E. Itkis, R.C. Haddon, S. Niyogi, Chemistry of single-walled carbon nanotubes, Acc. Chem. Res. 35 (2002) 1105–1113.
[22] V. Sadhu, N.A. Nismy, A.A.D.T. Adikaari, S.J. Henley, M. Shkunov, S.R.P. Silva, Nanotechnology 22 (2011) 265607.
[23] A.T. Mallajosyula, S.S.K. Iyer, B.J. Mazhari, Role of single walled carbon nanotubes in improving the efficiency of poly-(3-hexylthiophene) based organic solar cells, Appl. Phys. 108 (2012) 094902.
[24] A. Javier, B. Werner, Enhanced device performance using different carbon nanotube types in polymer photovoltaic devices, Carbon 46 (2008) 2067–2075.
[25] N.A. Nismy, A.A.D.T. Adikaari, S.R.P. Silva, Functionalized multiwall carbon nanotubes incorporated polymer/fullerene hybrid photovoltaics, Appl. Phys. Lett. 97 (2010) 033105.
[26] D. Gupta, M. Bag, K.S. Narayan, Correlating reduced fill factor in polymer solar cells to contact effects, Appl. Phys. Lett. 92 (2008) 093301.
[27] L.M. Andersson, C. Müller, B.H. Badada, F. Zhang, U. Würfel, O. Inganäs, Mobility and fill factor correlation in geminate recombination limited solar cells, J. Appl. Phys. 110 (2011) 024509.

Please cite this article in press as: R. Bhatia, L. Kumar, Functionalized carbon nanotube doping of P3HT:PCBM photovoltaic devices for enhancing short circuit current and efficiency, Journal of Saudi Chemical Society (2016), http://dx.doi.org/10.1016/j.jscs.2016.11.003